International Conference on Computational Fluid Dynamics (ICCFD11), Maui Hawaii, July 11-15, 2022 **ICCFD11-2022-2101**

Pseudo-boiling of supercritical water

R. Barney[a]*, R. Nourgaliev[a], R. McCallen[a], and J.P. Delplanque[b]
Corresponding author: rebecca.barney@ll.mit.edu

[a] Lawrence Livermore National Laboratory †
[b] University of California, Davis

Abstract: Supercritical fluid presents highly varying properties which contribute to unstable fluid dynamics and interesting heat transfer characteristics. At different isobaric pressures above the fluid's critical pressure, the property variations induce the fluid to transition from liquid-like to gas-like behavior. This investigates numerically the natural convection cavity with supercritical water and the influence of the large property variations on the flow field. In particular, the heated natural convection cavity is studied to determine where pseudo-boiling may occur. Results show that a high-fidelity simulation method developed at Lawrence Livermore National Laboratory can capture the extremely varying properties, unstable structures, and transition from liquid-like to gas-like in the supercritical fluid regime.

Keywords: Supercritical fluid, hydrodynamic instabilities, pseudo-boiling, high-order, fully-implicit

1 Introduction

The behavior of fluids at supercritical thermodynamic conditions is inherently complex due to large variations in thermodynamic and transport properties. The large property variations at, and above, the critical point are characteristic of supercritical fluids. For water, the critical point is defined as the end of the gas-liquid coexistence line, is at 647 K and 22.096 MPa (Figure 1c). Above this point at higher pressures and temperatures the fluid is in a supercritical state.

Numerical and experimental investigations for a variety of applications illustrate ongoing interest for these high-pressure, high-temperature fluids, especially for supercritical CO_2 and supercritical water. Some applications include microchannels for cooling (cryogenics), chemical extraction, and cooling for power generation [2, 3, 4].

With the use of supercritical fluids, the amount of heat transfer is directly associated with the large property variations, like the thermal diffusivity, viscosity, and specific heat, as seen in Figure 1a and b. The changes in the properties with temperature greatly affect the heat transfer from what is normally expected with single-phase fluids. Supercritical fluid benefits have traditionally been tied to the single-phase and high heat capacity nature of the fluid, however research has now suggested the existence of pseudo-two phases above the critical point [5]. The pseudo-two phase transition from liquid-like to gas-like is defined by the peaks of the specific heat, which occur at temperatures known as pseudo-critical temperatures. These peaks form a line known as the pseudo-critical or Widom line [5]. Seen in Figure 2 is the specific heat (in blue) and the density (in red) at various constant pressures with the specific heat maxima forming the Widom line.

Fluid properties crossing through the Widom line is akin to crossing the gas-liquid coexistence line below the critical point. Phase change below the critical point is characterized by a large, discontinuous jump in the enthalpy, corresponding to the latent heat. Phase change occurs at a constant temperature and a change in energy (release for condensation and uptake for evaporation). As a fluid crosses the Widom line a similar

*R.Barney is currently an MIT Lincoln Laboratory employee. No Laboratory funding or resources were used to produce the results/findings reported in this publication

†This work was performed under the auspices of the U.S. Department of Energy by Lawrence Livermore National Laboratory under Contract DE-AC52-07NA27344. Information management release number LLNL-CONF-836643.

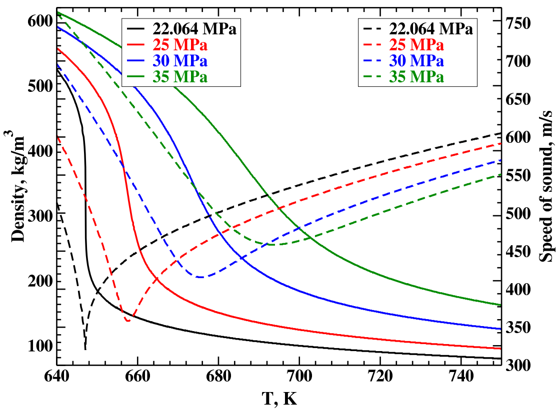

(a)

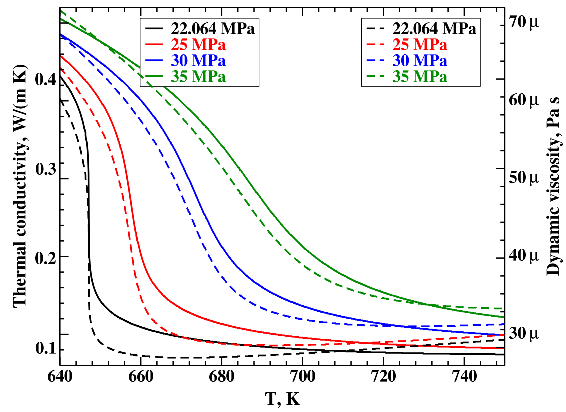

(b)

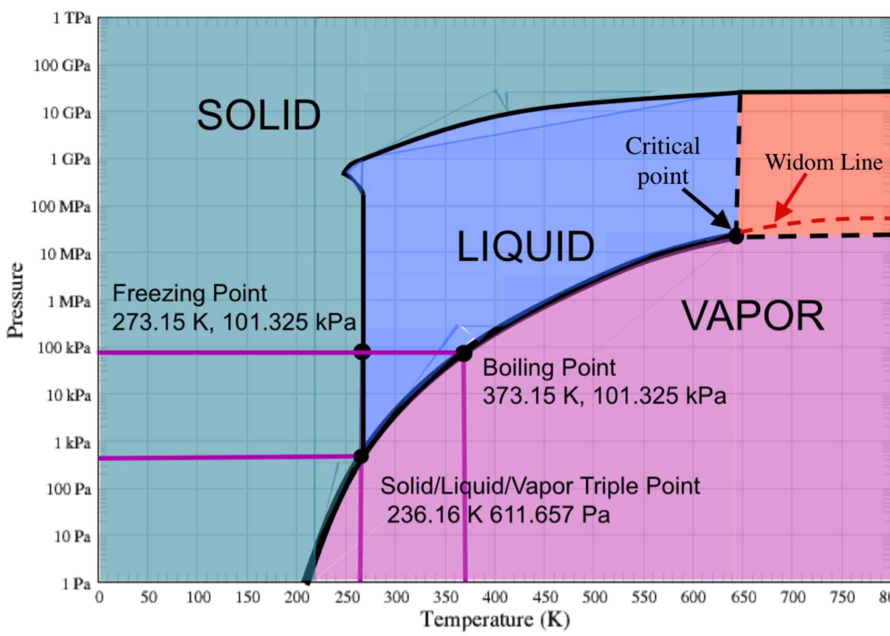

(c)

Figure 1: Plots (a,b) show the temperature dependence of material properties for water, through selected pressures above critical point, based on IAPWS-IF97 [1]. Plot (c) shows the phase diagram of water where the critical point and the Widom line provided.

transition of energy occurs, however, the transition is smooth and results in large, continuous variations in properties. Figure 3 shows the enthalpy versus temperature where the temperature at the critical pressure (blue line) is nearly constant during the energy (phase) change.

Similar to fluid properties below the critical point, crossing the Widom line is like transition from a liquid to a gas. This phase transition of liquid to gas can create boiling. A typical boiling curve can be seen in Figure 4. Fluid transitions through natural convection on to nucleate boiling where bubbles are formed, and then transitions to boiling where larger bubbles form and carry heat away from the heated surface until the critical heat flux is reached. At this point, film boiling occurs and a gaseous layer of fluid appears. Heat is then conducted through the gas film while the liquid evaporates at the interface [6, 7].

A boiling curve has yet to be extensively studied with supercritical fluids. An empirical and analytical study on the Widom line was described in 2015, in which Banuti [8] discussed the fluid transition across the

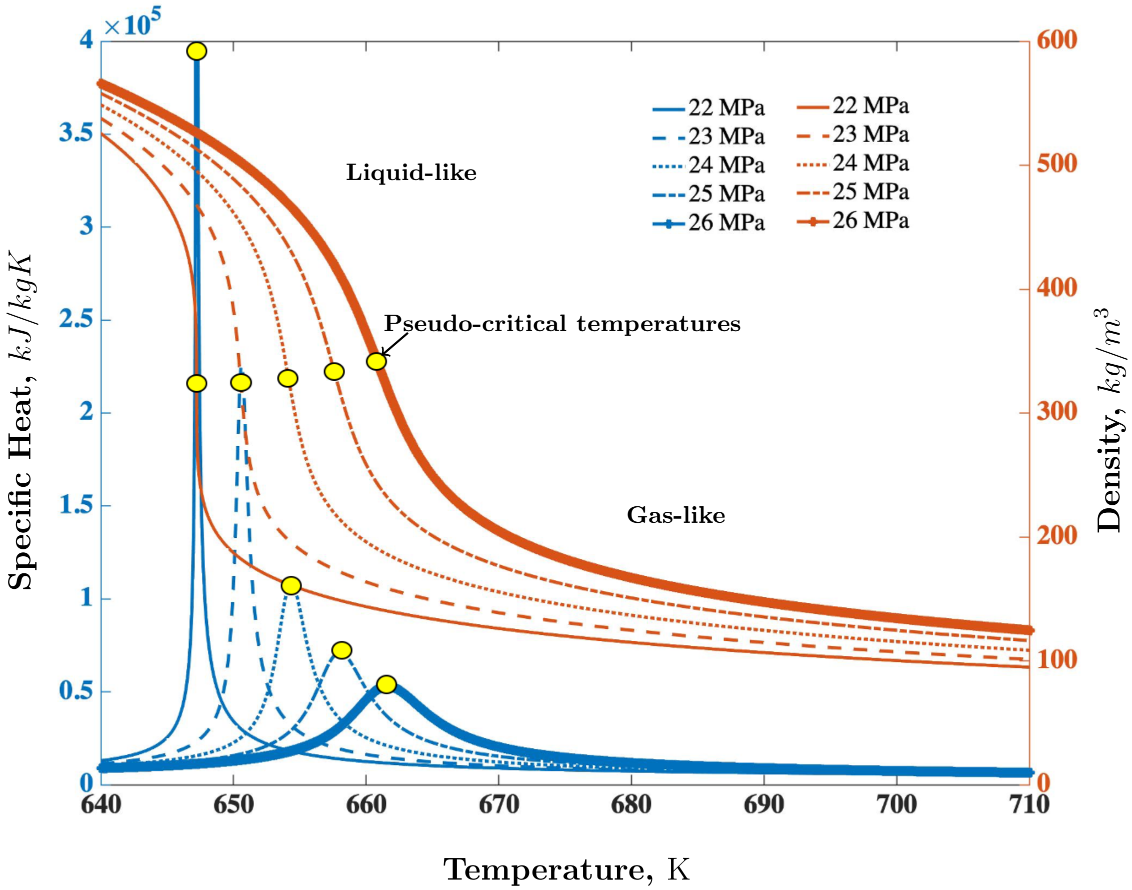

Figure 2: Specific heat and density versus temperature for various pressures. At 22 MPa is the critical temperature, and all other pressures are above the critical point. The yellow markers signify the pseudo-critical temperatures, and positions for the specific heat and the density.

Widom line. It was shown that pseudo-boiling exists due to the drastic variation in density and specific heat. Banuti stated that the *"... associated massive reduction in density and high specific heat capacity strongly resemble classical subcritical vaporization."* [8]. Further investigations by various authors such as Simeoni et al., Bolmatov et al., Frenkel et al., and Corrandi et al., have studied the pseudo-critical region and found that a cross-over state does exist [5, 9, 10, 11]. A film-like layer forming along walls of heated pipes or channels, noting that this film can be attributed to the large property variations and pseudo-boiling phenomena [12]. Similar to gaseous layers in film boiling, the pseudo-film can prevent heat from leaving the pipe through the walls creating heat transfer deterioration (HTD).

In this paper, a supercritical water natural convection cavity with a heated bottom wall is simulated to examine the formation of a pseudo-boiling curve. Calculation of the heat flux in the supercritical natural convection cavity allows for a comparison with the well-known boiling curve below the critical point.

To investigate the natural convection cavity, a high-order, fully-implicit, numerical method is used. The strong variations in thermophysical properties (in particular, density) are difficult to simulate and an altogether compressible framework is needed. Therefore, the compressible Navier-Stokes equations are solved without any assumptions. The fully-implicit, high-order in space and time, reconstructed discontinuous Galerkin (rDG) method is used and implemented within the multi-physics code called ALE3D developed at Lawrence Livermore National Laboratory (LLNL) [13].

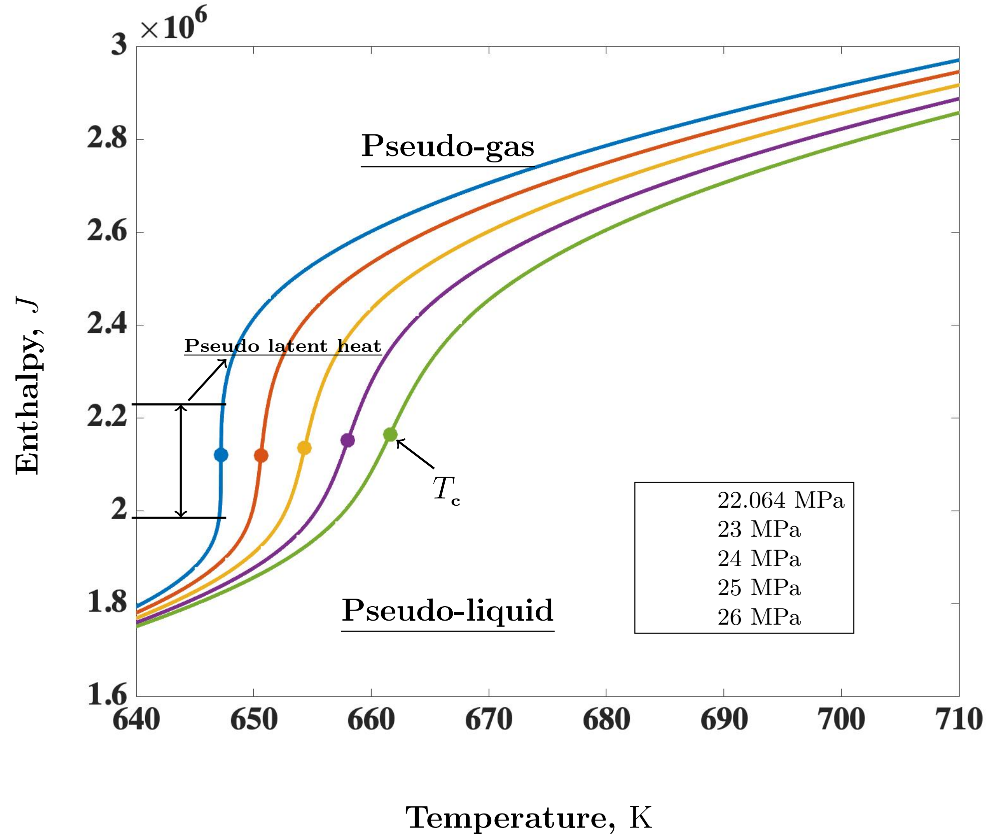

Figure 3: Enthalpy versus temperature, for selected pressures. The pseudo-phase transition is at the temperature where the isobaric specific heat has its maximum, i.e. at the Widom line.

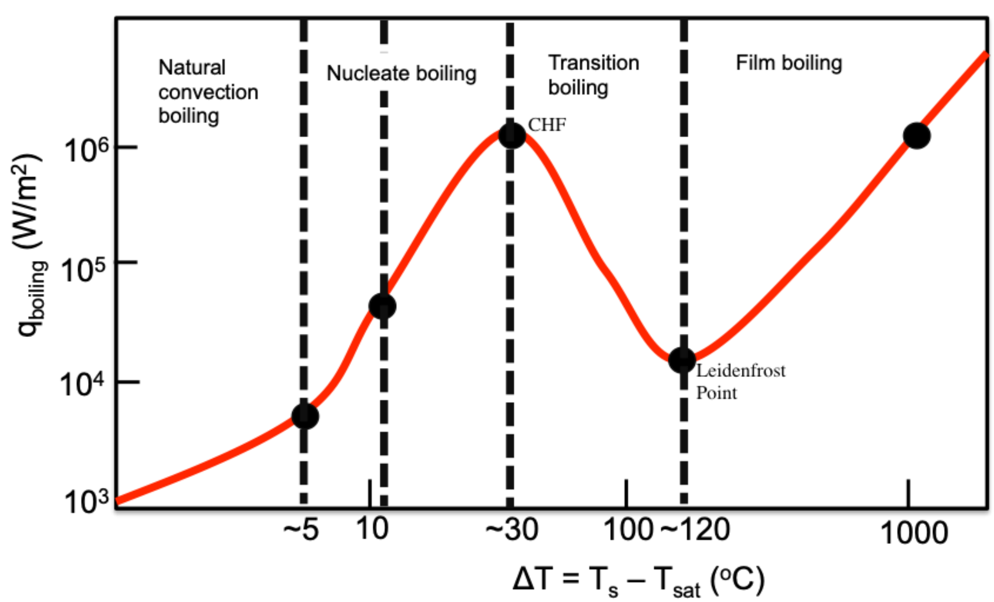

Figure 4: Sub-critical boiling curve for water where CHF is the critical heat flux and the Leidenfrost point is the minimum heat flux.

2 Mathematical Model and Numerical Method

This section describes the governing equations and constitutive relations utilized for the simulations. The equation of state for water brings many challenges, due to the highly varying properties. The large density variations with temperature ensure a compressible flow, but the low speed, low-Mach number flow induces challenges. In this work, the fully compressible flow equations are used along with the reconstructed Discontinuous Galerkin (rDG) approach for discretizing the fully-implicit, Newton-Krylov based procedure. The method is implemented in the Multiphysics code, ALE3D, at LLNL [13].

The governing equations are the Navier-Stokes and energy equations. It is instructive to note that the Boussinesq approximation for gravitational forces is not used due to the large density variations with temperature. For details on the equations please see Nourgaliev et al. [14]. It is essential to properly scale the governing equations to ensure viability of non-linear and linear solvers involved in the Newton-Krylov-based fully-implicit framework. The scaling parameters used for this work can be seen in detail in Nourgaliev et al. and Barney et al. [14, 15].

The final non-dimensional equations used are the following.

$$\begin{aligned} &\underline{\text{Mass conservation}} \\ &\partial_{\hat{t}} \hat{\rho} + \partial_{\hat{j}} \left(\hat{\rho} \hat{\mathbf{v}}_j \right) = 0, \\ &\underline{\text{Momentum conservation}} \\ &\partial_{\hat{t}} \hat{\rho} \hat{\mathbf{v}}_i + \partial_{\hat{j}} \left(\hat{\rho} \hat{\mathbf{v}}_i \hat{\mathbf{v}}_j + \tilde{P} - \tilde{\boldsymbol{\tau}}_{i,j} \right) = \tilde{\mathbf{g}}_i \left(\hat{\rho} - \hat{\rho}_h \right), \end{aligned} \tag{1}$$

and

$$\begin{aligned} &\underline{\text{Total energy conservation}} \\ &\partial_{\hat{t}} \hat{\rho} \hat{e} + \partial_{\hat{j}} \left(\left[\hat{\rho} \hat{e} + \epsilon_{\mathrm{E}} \left(\hat{P}_R + \tilde{P} - \tilde{\boldsymbol{\tau}}_{i,j} \right) \right] \hat{\mathbf{v}}_j + \tilde{\mathbf{q}}_j \right) = \hat{q}_v + \epsilon_{\mathrm{E}} \hat{\mathbf{v}}_k \tilde{\mathbf{g}}_k \left(\hat{\rho} - \hat{\rho}_h \right) \ , \end{aligned} \tag{2}$$

where the dimensionless variables are defined as:

$$\begin{gathered} \hat{t} = \frac{t}{\bar{t}},\ \hat{\mathbf{x}} = \frac{\mathbf{x}}{L},\ \hat{\rho} = \frac{\rho}{\bar{\rho}},\ \hat{\rho}_h = \frac{\rho_h}{\bar{\rho}},\ \hat{\mathbf{v}} = \frac{\mathbf{v}}{\bar{\mathrm{V}}},\ \hat{P}_R = \frac{P_R}{\bar{P}}, \\ \tilde{\mathbf{g}}_i = \frac{L|g|}{\bar{v}^2} \hat{\mathbf{g}}_i,\ \ \hat{\mathbf{g}}_i = \frac{\mathbf{g}_i}{|g|},\ \tilde{T}_h = \frac{T_h - T_R}{\bar{T}}, \\ \hat{\mu} = \frac{\mu}{\bar{\mu}},\ \tilde{\mu} = \frac{\hat{\mu}}{f_{\mathcal{M}} Re},\ \hat{\boldsymbol{\tau}} = \frac{\boldsymbol{\tau} L}{\bar{\mu} \bar{\mathrm{V}}},\ \tilde{\boldsymbol{\tau}} = \frac{\hat{\boldsymbol{\tau}}}{f_{\mathcal{M}} Re}, \\ \hat{e} = \frac{e}{\bar{\mathrm{u}}},\ \hat{C}_p = \frac{C_p}{\bar{C}_p},\ \hat{\kappa} = \frac{\kappa}{\bar{\kappa}},\ \tilde{\kappa} = \frac{\hat{\kappa}}{f_{\mathcal{M}} Pe}, \\ \hat{\mathbf{q}}_j = \frac{\mathbf{q}_j L}{\bar{\kappa} \Delta T},\ \tilde{\mathbf{q}}_j = \frac{\hat{\mathbf{q}}_j}{f_{\mathcal{M}} Pe},\ \hat{q}_v = \frac{q_v L}{\bar{\rho} \bar{\mathrm{V}} \bar{\mathrm{u}}}, \end{gathered} \tag{3}$$

where ϵ_{E} is a scaling parameter representing the ratio of kinetic and thermal energies:

$$\epsilon_{\mathrm{E}} = \frac{\bar{\mathrm{V}}^2}{\bar{\mathrm{u}}}, \tag{4}$$

which appears in the energy equations as a factor for the viscous heating and pressure/body force work terms. Thus, the total energy can be represented as follows:

$$\hat{e} = \hat{\mathrm{u}} + \epsilon_{\mathrm{E}} \frac{\hat{\mathbf{v}}^2}{2}. \tag{5}$$

To discretize nonlinear mixed hyperbolic-parabolic systems of governing equations, the reconstructed Discontinuous Galerkin (rDG) method is used. This method was originally introduced in [16]. A term $\mathrm{P}_n\mathrm{P}_m$ Discontinous Galerkin was formed, where P_n refers to the sovled-for degrees of freedom, while P_m is reconstructed and defines the overall accuracy of the method. More details on the method can be found in [17]. This algorithm allows for a coarser mesh while still resulting in a high-order solution. The method-of-lines diagonally implicit Runge-Kutta (DIRK) time discretization of equation is used.

A necessary step for the simulations is implementing an equation of state (EoS) for supercritical water. In this work the IAPWS was used, which provides equations to model water in different temperature and pressure regimes [1, 18, 19]. The core equation for the region of interest is defined as the following.

$$\phi(\delta,\tau) = \frac{(\rho,T)}{RT} = n_1 \ln\delta + \sum_{i=2}^{40} n_i \delta^{I_i} \tau^{J_i} \tag{6}$$

Where the dimensionless density, δ, and temperature, τ are defined as $\delta = \rho/\rho_c$, and $\tau = T_c/T$. The pressure is calculated as a function of density and temperature.

$$\frac{p(\delta,\tau)}{\rho RT} = \delta\phi_\delta \tag{7}$$

The first and second derivatives of the core equation relative to density and temperature are used to evaluate all other thermodynamic and transport properties. Special care was taken to properly represent and incorporate the EoS in the high-order, fully-implicit technique, as the solution of these thermodynamic properties might become prohibitively expensive for the global non-linear solver. The computations have been optimized to be compatible with the DG based residual evaluations where the non-linear solver is formulated in terms of DG degrees of freedom for the dimensionless pressure, velocity, and temperature. A Newton solver is required to evaluate density before evaluating the remaining thermodynamic variables. A quadruple precision (16-bit) is used for evaluation of the properties as it was found that this improves the conditioning and overall convergence of the Newton-Krylov algorithm. The performance of the non-linear solver using the optimized EoS is comparable (only 2-3 times more expensive) to the performance of the solver employed with a simpler analytic EoS.

3 Problem set up

To investigate natural convection, a 2D cavity is simulated, as seen in Figure 5. The initial temperature is uniform at 650 K while the bottom wall is heated at a constant temperature greater than pseudo-critical of 658.5 K at a constant 25 MPa pressure. The sidewalls are adiabatic and the top wall is maintained at the initial temperature. No slip conditions are used for the top, bottom, and side walls. A pressurizer is used at the top wall to maintain a constant pressure within the cavity. The pressurizer allows for the fluid to expand due to heating while also keeping the constant pressure within the cavity.

The heated bottom wall is kept constant at various temperatures hotter than the initial temperature, starting at 660 K and going up to 710 K. The initial Rayleigh number of 1×10^7 is used to vary the amount of buoyancy in the flow field. The mesh used for all results is seen in Figure 5. A mesh convergence study was performed proving results are valid for these simulations [15].

4 Results and Discussion

Results demonstrate the ability of the simulation method to capture the pseudo-two-phase regime, and Widom line accurately. The natural convection cavity simulation with a heated bottom wall can be seen in Figure 6 where the pressurizer has been removed for visualization. The top left figure has a wall temperature of 670 K, while the bottom right has a wall temperature of 700 K. The figures show the local Rayleigh number giving insight into the buoyancy forces present in the flow field. The heated fluid at the bottom of the cavity is driven upwards by buoyancy forces of lighter, less dense fluid mixing with the heavier, denser fluid in the mid-cavity. Mixing appears as the density changes. A lower temperature delta (temperature of wall – temperature of bulk) results in less mixing, as expected, seen with the temperature delta of 20. At the highest temperature delta of 50, the pseudo-phase transition line can be seen in red, where the fluid near the wall is pseudo-gas and that in the bulk flow is pseudo-liquid. It is apparent that a pseudo-film appears at the bottom heated wall of the cavity, especially for the higher wall temperatures. The sudden density change with temperature allows for lighter fluid to mix into the center of the cavity and tend to behave similar to bubbles. As the temperature along the bottom wall increases, the pseudo-bubbles increase in quantity, and size, and therefore increase the mixing.

Another measure of buoyancy and mixing is the local Rayleigh number, seen in Figure 6. The inlet Rayleigh number for these simulations was 1×10^7 however, it can be seen that the local Rayleigh number

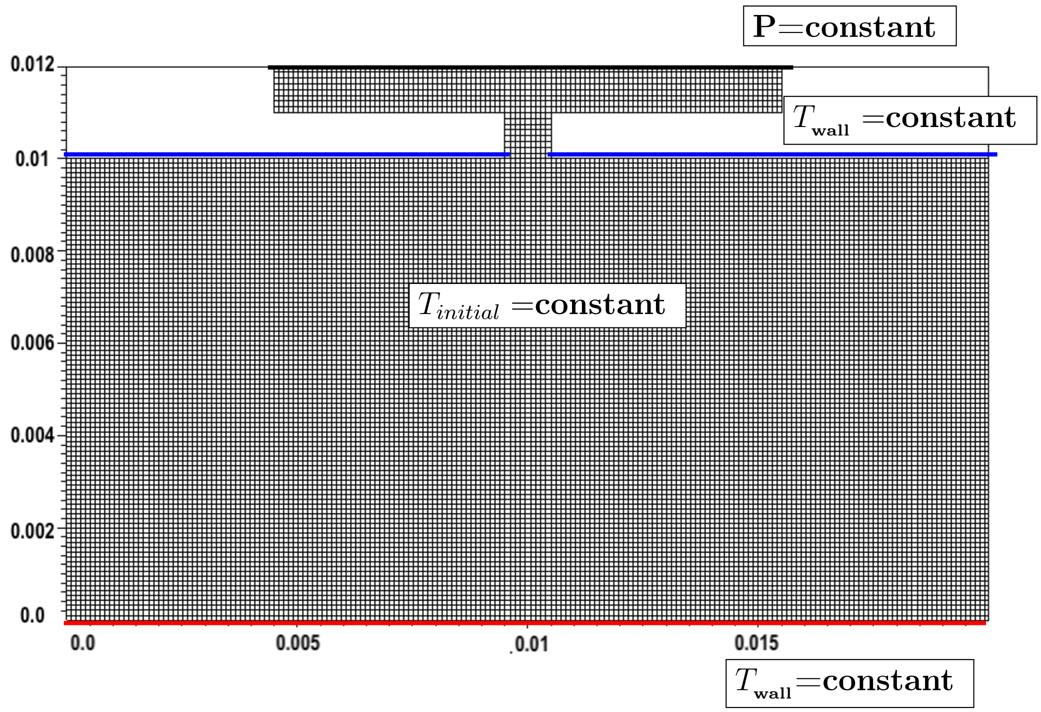

Figure 5: Simulation geometry, where the bottom wall is heated at a constant temperature greater than the initial cavity temperature. The walls are adiabatic, and no-slip. A constant pressure is provided at the top of th pressurizer. A constant initial Rayleigh number is provided for all simulations.

varies through the cavity and is smaller in the middle than at the edges/bottom. The viscosity and the thermal conductivity both decrease as the temperature increases, therefore increasing the local Rayleigh number. As the local Rayleigh number increases and the wall temperature is increased, the Widom line moves further into the cavity showing that both pseudo-liquid and pseudo-gas coexist in this flow regime, as seen in the zoomed in figure.

Due to the existence of both phases it is natural to question, if there a boiling curve in this fluid regime. The natural convection cavity with a temperature boundary condition allows for calculation of the heat flux, and therefore a potential boiling-like curve. The heat flux was calculated from the following equation, $q_{wall} = h_{wall} \times (T_{wall} - T_{sat})$, and the heat transfer coefficient was determined from the Nusselt number and thermal conductivity.

For this analysis T_{sat} was set as the pseudo-critical temperature of 658.5 K. The heat transfer coefficient was calculated from $H_{wall} = Nu\frac{k}{A}$. To get a singular value for each simulation, the Favre-averaged heat flux at the bottom wall over space and time was calculated.

Visually, as seen in Figure 6, with a small delta temperature there are little, to no plumes that develop. The Widom line is barely reached with this small temperature delta. Further, the density remains more constant in the cavity as compared to a higher temperature delta. The gas-like layer is almost undetectable, and the flow appears to be in the natural convection regime only. As the wall temperature increases the unstable features grow, the gas-like film layer grows, and more mixing occurs. A thicker gas-like film layer appears and remains even as some of the gas-like fluid detaches into the bulk of the cavity. Similar to the boiling regimes observed below the critical point, lower temperatures correspond to lower heat flux. Importantly in the supercritical flow there is no evident nucleation process. The pseudo-gas film becomes thick and unstable plumes are driven off the bottom surface which instigate the pseudo-boiling phenomenon. As the wall temperature increases to about 680K a peak in the heat flux appears, seen in Figure 7. As the wall temperature grows pseudo-gas 'puffs' start to pull off the wall carrying heat away, mixing with the pseudo-liquid fluid, and therefore increasing the heat flux again.

A pseudo-boiling curve created from the simulations with increasing wall temperature can be seen in

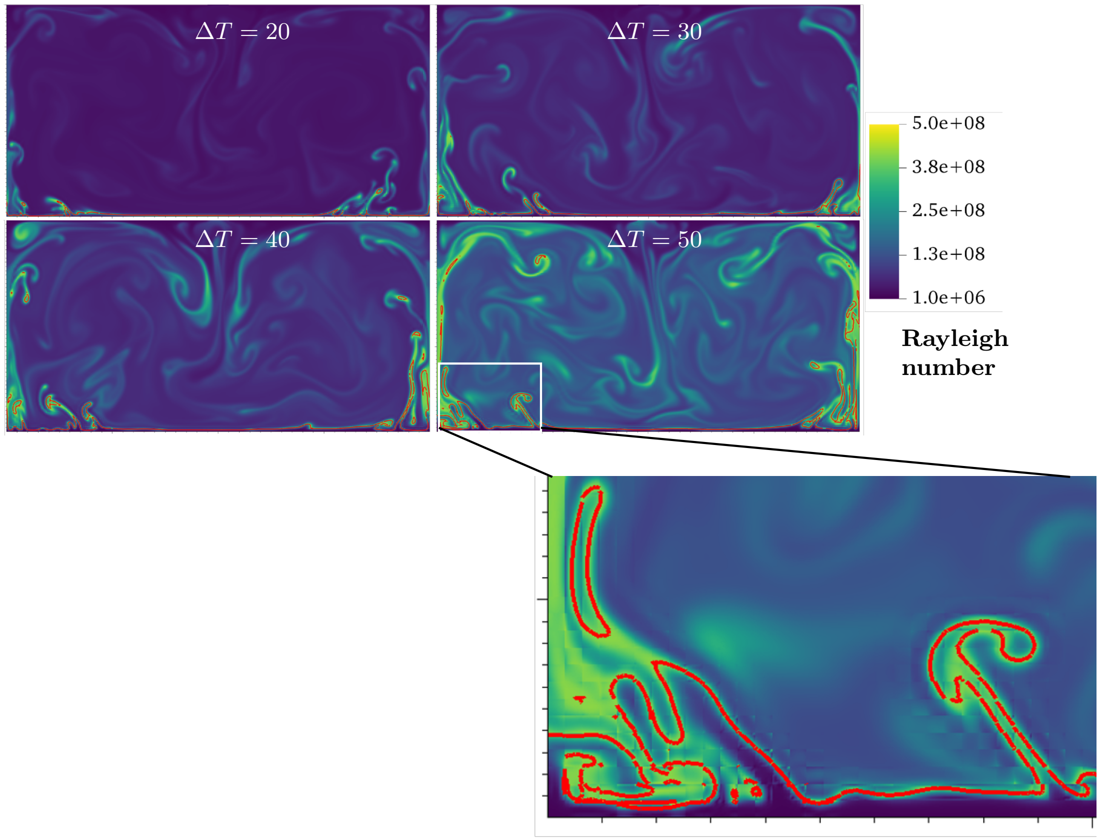

Figure 6: Colormap of Rayleigh number with the Widom line drawn in red. The wall temperature is increased from 660 K to 700 K.

Figure 7. It is clear that as the wall temperature increases so does the heat flux. An increase in heat flux with temperature shows a local maximum (akin to the critical heat flux) followed by a decrease to a local minimum (akin to the Leidenfrost point) followed by a film boiling like regime where the wall heat flux increases with wall temperature. The potential of a minimum heat flux, where a film layer becomes larger and more stable, is seen at $\Delta T = 20K$ (wall temperature of 680 K). As the wall temperature increases that the gas-like layer can maintain a substantial thickness while also allowing gas-like puffs to break off of the bottom surface. The gas like puffs remove some heat from the film layer at the wall, increasing the mixing in the cavity, and subsequently increasing the heat flux again.

5 Conclusion and Future Work

It is apparent that a pseudo-phase transition occurs in the supercritical thermodynamic regime. The transition can be captured with a high-order, fully-implicit code developed at LLNL. The pseudo-phase transition is demonstrated with a natural convection cavity where the higher the delta temperature between the saturation temperature and the wall temperature induces more mixing, the generation of a thicker gas-like film, and potential pseudo-boiling. The resulting pseudo-boiling curve illustrates similarities with the boiling curve below the critical point. To confirm this phenomenon more simulations must be completed at intermediate wall temperatures, and high wall temperatures, to determine the behavior of the heat flux. It would be wise to complete simulations with a heat flux boundary condition as well and calculate the wall temperature to a create a pseudo-boiling curve.

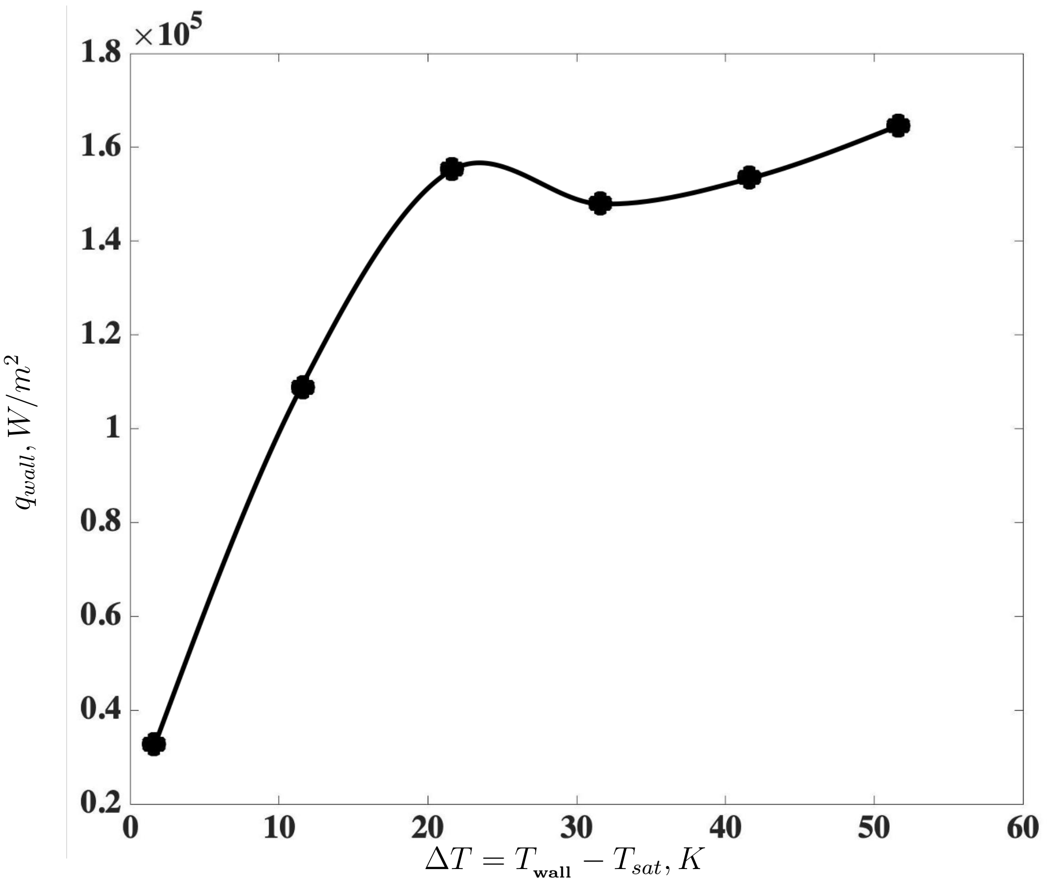

Figure 7: Pseudo-boiling curve calculated for various wall temperature simulations.

References

[1] J. R. Cooper and Dr. R.B. Dooley. The international association for the properties of water and steam. Revised release, University of London, and Structural Integrity Associates, Lucerne, Switzerland, August 2007.

[2] Luisa F. Cabeza, Alvaro de Gracia, A. Inés Fernández, and Mohammed M. Farid. Supercritical co2 as heat transfer fluid: A review. *Applied Thermal Engineering*, 125:799–810, July 2017.

[3] R. Camparelli an L. Baldino and E. Reverchon. Supercritical fluids applications in nanomedicine. *The Journal of Supercritical Fluids*, 101:193–214, March 2015.

[4] Catherine Kelly and Steve Howdle. Supercritical processing, 2008.

[5] G.G. Simeoni, T. Bryk, F. A. Borelli, M. Krisch, and et. al. The widom line as the crossover between liquid-like and gas-like behavior in supercritical fluids. *Nature Physics*, 6:503–507, July 2010.

[6] Warren M. Rohsenow. Boiling. *Annual Review of Fluid Mechanics*, 3:211–236, 1971.

[7] P.B. Whalley. *Boiling, Condensation, and Gas-Liquid Flow*. Oxford University Press, 1987.

[8] D.T. Banuti. Crossing the widom-line - supercritical pseudo-boiling. *The Journal of Supercritical Fluids*, January 2015.

[9] Dima Bolmatov, V.V. Brazhkin, and K. Trachenko. Thermodynamic behaviour of supercritical matter. *Nature communications*, August 2013.

[10] Kanka Ghosh and C.V. Krishnamurthy. Frenkel line crossover of confined supercritical fluids. *Scientific Reports*, 2019.

[11] P. Gallo, D. Corrandini, and M. Rovere. Widom line and dynamical crossovers as routes to understand supercritical water. *Nature Communications*, December 2014.

[12] M. Sharabi and W. Ambrosini. Discussion of heat transfer phenomena in fluids at supercritical pressure

with the aid of cfd models. *Annals of Nuclear Energy*, 36:60–71, December 2009.

[13] A. Nichols and et al. ALE3D users manual, an arbitrary lagrangian/eulerian 2d and 3d code system. Technical report, Lawrence Livermore National Laboratory, 2014.

[14] R. Nourgaliev, P. Greene, B. Weston, R. Barney, A. Anderson, S. Khairallah, and J. P. Delplanque. High-order fully implicit solver for all-speed fluid dynamics. *Shock Waves*, pages 1–39, 2018.

[15] Rebecca Barney, Robert Nourgaliev, Rose McCallen, and J.P. Delplanque. Heat transfer and pseudo phase transistion for low-reynolds, mixed-convection channel flow in the supercritical thermodynamic regime. *International Journal of Heat and Mass Transfer*, October 2021.

[16] H. Luo, L. Luo, R.R. Nourgaliev, and V. Mousseau. A Reconstructed Discontinuous Galerkin method for the compressible Euler equations on arbitrary grids. In *19th AIAA Computational Fluid Dynamics Conference*, San Antonio, Texas, USA, June 22-25 2009. AIAA 2009-3788.

[17] H. Luo, L. Luo, R.R. Nourgaliev, and V. Mousseau. A Reconstructed Discontinuous Galerkin method for the compressible Navier-Stokes equations on arbitrary grids. 229:6961–6978, 2010.

[18] Karol Daucik and Dr. R.B. Dooley. The international association for the properties of water and steam: Release on the iapws formulation 2011 for the thermal conductivity of ordinary water substance. Release, Larok s.r.o., Plzen, Czech Republic, September 2011.

[19] J. R. Cooper and Dr. R.B. Dooley. The international association for the properties of water and steam: Release on the iapws formulation 2008 for the viscosity of ordinary water substance. Release, University of London, and Structural Integrity Associates, Berlin, Germany, September 2008.